Fabrication and Characterization of Lead Sulphide Colloidal Quantum Dot Photodetectors for the Near Infrared

L. Colace, A. De Iacovo, C. Venettacci and S. Bruno
Department of Engineering, University Roma Tre, Via Vito Volterra 62, Rome, Italy

Keywords: Colloidal Quantum Dots, Optoelectronic Devices, Photodetectors, Solution-processed Nanomaterials.

Abstract: Colloidal quantum dots are attracting a lot of interest for the fabrication of optoelectronics devices. In particular, they are suitable for simple, low cost and efficient photodetectors. Here we report on our recent results on lead sulphide colloidal quantum dot photoconductors operating in the near infrared spectral range. We describe the device fabrication process and provide an exhaustive electrical and optical characterization. The photodetectors exhibit a responsivity as high as 46 A/W and specific detectivity of about $1.7 \cdot 10^{11}$ $cmHz^{1/2}W^{-1}$. Performance are investigated as a function of the voltage bias, device geometry and optical power. An evaluation of the device stability over time was also carried out.

1 INTRODUCTION

Colloidal quantum dots (CQD) are semiconductor nanocrystals that are synthesized and suspended in solution. Their typical size between 2 and 10 nm produces three-dimensional quantum confinement, enabling band-gap engineering and dramatically enhancing optical emission and absorption with tunable spectra provided by the quantum size effect (Weidman et al., 2014).

Since the hot-injection method was first proposed (Murray et al., 1993), nanoparticle diameters sizable over more than one decade with less than 5% standard deviation can be easily obtained, providing precise and repeatable characteristics (Moreels et al., 2009). As-synthesized CQDs are typically coated with ligand molecules in order to prevent aggregation and precipitation. Such long ligands typically produce too large inter-dot spacings preventing the carrier transport. Therefore, in order to make the CQD suitable for optoelectronic devices, the replacement of long molecules with shorter ones is required. In addition, such surface processing introduces useful changes in the nanoparticle properties adding further degrees of engineering (Garcia De Arquer et al., 2015). Due to their solution processability, CQDs allow simple, low temperature fabrication and are compatible with several substrates, including polymers, glass and silicon (Saran and Curry, 2016). Thanks to their unique electronic and optical properties and their simple fabrication process, CQDs have attracted lot of interest for a wide variety of optoelectronic devices, including light emitting diodes (Gong et al., 2016), photodetectors (Garcia De Arquer et al., 2017) and solar cells (Kim et al., 2013). Fig.1 shows the emission tunability of the most common CQDs, with operating wavelengths spanning from the bulk material band gap down to the shortest confinement-induced blue shifted emission.

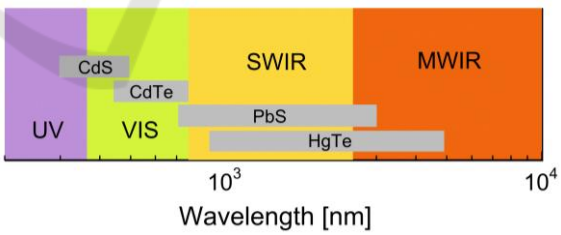

Figure 1: Emission tunability of selected semiconductor CQDs. Ultraviolet (UV), visible (VIS), short wavelength infrared (SWIR) and medium wavelength infrared (MWIR) are also indicated.

Lead sulphide (PbS) CQDs are the most advanced colloidal material for the near infrared (NIR) in terms of both monodispersion and reproducibility and several photodetectors have been proposed and demonstrated resorting to different device architectures, including photodiodes, phototransistors and photoconductors (Saran et al.,

Colace, L., De Iacovo, A., Venettacci, C. and Bruno, S.
Fabrication and Characterization of Lead Sulphide Colloidal Quantum Dot Photodetectors for the Near Infrared.
DOI: 10.5220/0007412400790084
In *Proceedings of the 7th International Conference on Photonics, Optics and Laser Technology (PHOTOPTICS 2019)*, pages 79-84
ISBN: 978-989-758-364-3

2016). The latter are particularly interesting because of their large responsivity and simple fabrication process, suitable for integration with other technologies. PbS photoconductors have been also demonstrated in practical applications (Gao et al., 2014) (De Iacovo et al., 2017) (Venettacci et al., 2017). After the demonstration of very large NIR responsivity (>1000 A/W) and detectivity of PbS photoconductors (Konstantatos et al., 2006), several PbS CQD photoconductive detectors were proposed resorting to different approaches aimed at the improvement of the device performance (Saran et al., 2016). However, the best performance has been often obtained biasing the device at relatively high voltage, unpractical for several applications.

In this work we report on our recent results on PbS CQD photoconductors fabricated with a simple process based on ligand exchange and drop casting the sensitive material onto interdigitated contacts.

Our extensive device characterizations were focused in the low bias regime in dark and under optical excitation at 1.3 µm. Responsivity and detectivity were measured at different voltage bias and different optical power and for different device dimensions.

2 EXPERIMENTAL

The photoconductor devices were fabricated starting from a commercial 10mg/ml solution of PbS quantum dots capped with oleic acid and dispersed in toluene (Sigma-Aldrich 747076, with the first excitonic absorption peak at 1320 nm). In order to perform the required ligand exchange, CQD was centrifuged in methanol and dried in vacuum. Then, the nanoparticles were redispersed in octane at a concentration of 0.83 mg/mL. The CQD solution was drop-casted onto 1 mm^2 pre-patterned, interdigitated Ti-Au contacts deposited on SiO_2/Si commercially available substrates. The drop was dried, then followed by butylamine for ligand exchange until evaporation. Such deposition was repeated ten times in order to obtain a CQD film of about 500 nm. The devices were finally washed in methanol to remove the butylamine further reducing the interdot distance. Interdigitated contacts are provided with 1 mm^2 square bonding pads. Devices are available in 1 cm^2 silicon chips provided with 10 photodetectors. The schematic and geometry is reported in Fig.2. A more detailed description of the CQD processing and device fabrication can be found elsewhere (De Iacovo et al., 2016) (Stivala et al., 2007). With respect to previously reported fabrication procedures, we employed a hybrid technique, removing the long chain oleic acid in the liquid phase and then linking butylamine to PbS QDs directly on the deposition substrate. In this way, we keep the solution processing as simple and fast as possible but, at the same time, we limit the number of washing and soaking steps usually needed in solid-phase ligand exchange processes.

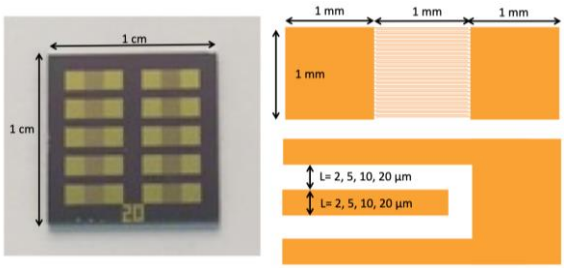

Figure 2: Photograph of the silicon chip with ten interdigitated contacts (left) and schematic of the contacts with dimensions.

The method used for the investigation was the measurement of the device current-voltage characteristics in dark and under illumination using a precision source-measure unit (Keithley 2612B). Device parameters such as dark current, responsivity and detectivity were measured for different interdigitated finger spacing, voltage bias and optical power. The optical source is a variable power semiconductor laser with a 1.31 µm emission. The spectral response was measured by a Jobin Yvon TRIAX 550 Spectrometer. The detectivity was evaluated by the measurement of the noise current performed using a FEMTO DLPCA-200 ultra-low noise current amplifier and a HP3588A spectrum analyzer. Finally, dark current and photocurrent measurements were taken over time in order to investigate the device temporal stability.

3 RESULTS AND DISCUSSION

A typical current-voltage plot for device with L=2 µm is reported in Fig. 3. A linear behavior confirming the ohmic behavior is observed, as expected from a photoconductor and typically observed in PbS CQD deposited on high work function metals such as Au (Voznyy et al., 2012). The typical device resistance R_d and dark current density J_d measured at 1V are about 360 kΩ and 0.28 mA/cm^2, respectively for L=2 µm. In the inset, the measured device resistance R_d is reported for different finger spacing.

The device spectral response at 1V bias is shown in Fig. 4 and compared with the optical absorption spectrum of the PbS solution before ligand exchange. The absorption peak at 1.32 μm is clearly visible and it is not shifted with respect to the absorption spectrum. The spectral response does not change significantly with bias.

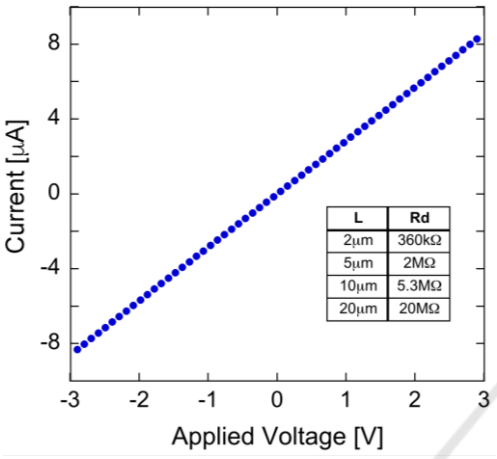

Figure 3: Current-voltage characteristic of a device with L=2 μm. The device resistance for different values of L is reported in the inset.

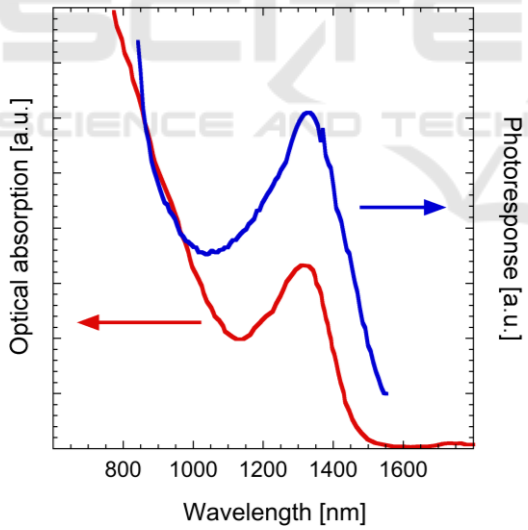

Figure 4: Typical spectral response at 1 V bias (blue) compared with the optical absorption spectrum of the PbS solution (red).

The responsivity is one of the most important characteristic of a photodetector as it is related to its quantum efficiency. Photoconductors typically exhibit large responsivity due to their intrinsic gain. It has been demonstrated that gain in PbS CQD photoconductors depends on the trap states present at the quantum dot surface (Konstantatos and Sargent, 2007). Fig.5 shows the detector responsivity R versus the finger spacing L at 1 V and 3 V bias as evaluated from the net current, according to the following equation:

$$R = \frac{I - I_{\mathrm{d}}}{P_{\mathrm{in}}} \qquad (1)$$

where I is the total current under illumination, I_d is the dark current and P_{in} is the optical input power. Our devices (L=2) exhibit a maximum responsivity of 46 A/W at 1.3 μm, 4 nW optical excitation and 3 V bias. Such performance is comparable with previously reported similar devices and compares favorably with most results reported at low applied voltage.

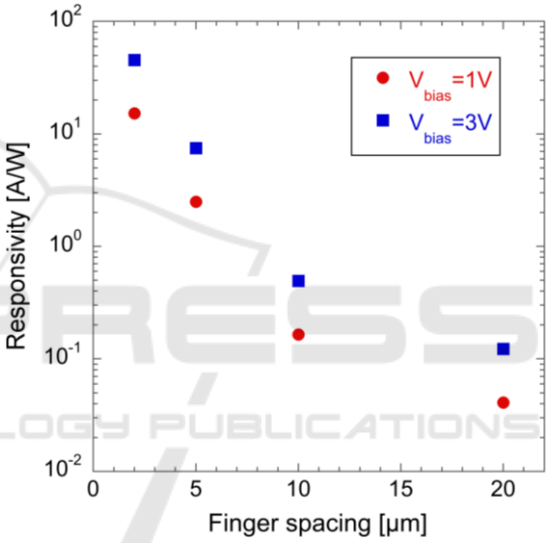

Figure 5: Responsivity for different finger spacing L at 1V (red) and 3V (blue) bias voltage measured at low optical power (4 nW).

We observe $R \propto L^{-2}$ and proportional to the applied voltage, as expected for common photoconduction. Unfortunately, the photoresponse is not linear with respect to the optical power. Fig. 6 plots the responsivity versus optical power for a 2μm spacing device biased at 1 V.

It exceeds 10 A/W below 200 nW with peak values >40 A/W in the nW range. The decrease of the responsivity with light intensity is typical of PbS CQD devices and it can be associated with the dependence of the occupancy of the mid-gap states (responsible for the gain) on light intensity (Konstantatos and Sargent, 2009).

Thanks to their large responsivity, CQD PbS photoconductors are very promising for several applications. However, they intrinsically suffer large

dark currents. Even if dark current can be subtracted, it produces noise that limits the detector sensitivity (Masini et al, 2004). The most common figure of merit for the evaluation of a photodetector sensitivity is the specific detectivity D^*, defined as follows:

$$D^* = \frac{R\sqrt{AB}}{i_n} \quad (2)$$

where R is the responsivity, A is the device area, B is the bandwidth and i_n is the noise current. B was measured by evaluation of the fall time following a step function while i_n was measured from the noise spectral density obtained by a spectrum analyzer (De Iacovo et al., 2017).

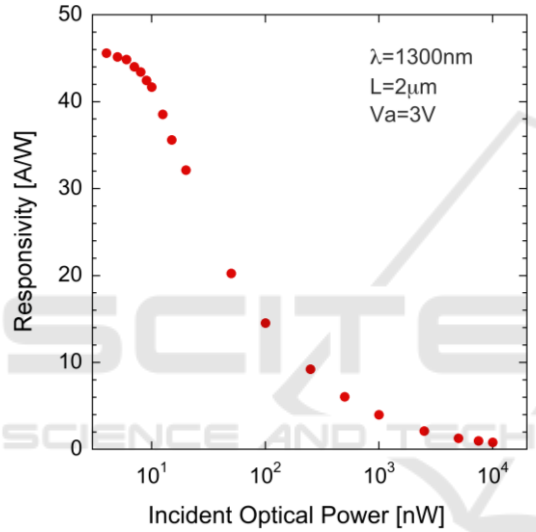

Figure 6: Responsivity versus optical power.

Fig. 7 shows the typical detectivity for different finger spacing. The larger detectivity for large L can be explained in terms of the greater decrease of the dark current with respect to the increase of the responsivity. In our detectors, D^* does not significantly change with the applied voltage. A maximum detectivity exceeding $1.7 \cdot 10^{11}$cmHz$^{1/2}$W^{-1} has been obtained.

It is known that CQDs based photodetectors suffer aging phenomena, due to surface reactions that can change the defect distribution and occupation responsible for the carrier transport (Hagfeldt et al., 1995).

Here, we report on a preliminary investigation of the temporal stability over 30 days carried out on as-deposited device compared to devices passivated with polydimethylsiloxane (PDMS) aimed at the reduction of CQD exposure through passivation.

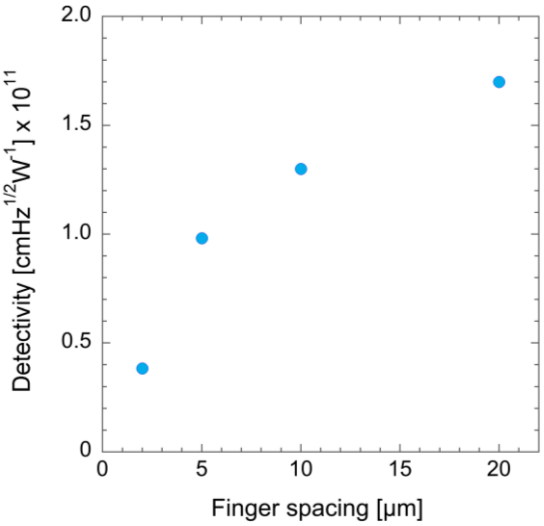

Figure 7: Detectivity for different finger spacing measured at low optical power (4 nW).

Fig. 8 and 9 shows the change of the normalized dark current and photocurrent, respectively. For both dark current and photocurrent the time drift is reduced in the case of the passivated devices.

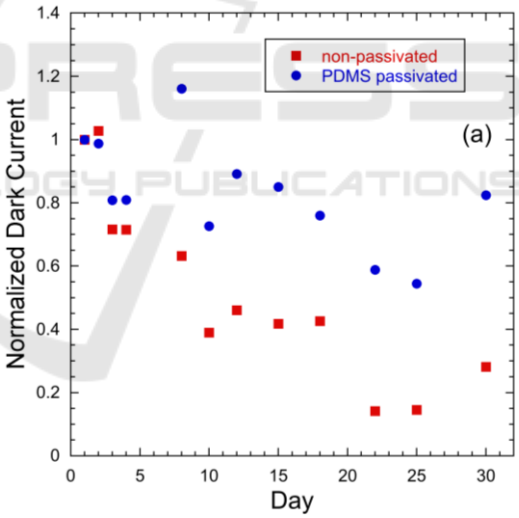

Figure 8a: Normalized dark current versus time.

The overall time behaviour can be better evaluated by the ratio between photocurrent and dark current reported in Fig. 8c. The passivated devices perform better even if they still exhibit a significant change. Alternative approaches are under investigation.

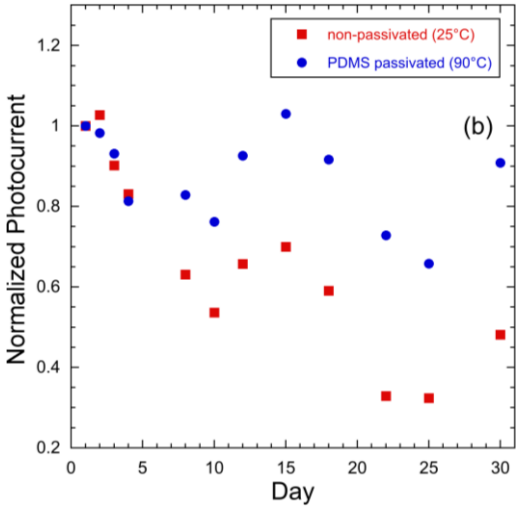

Figure 8b: Normalized photocurrent versus time.

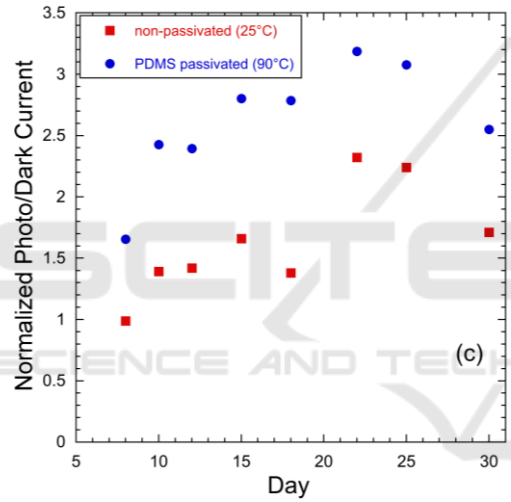

Figure 8c: Normalized photo/dark ratio versus time.

4 CONCLUSIONS

We have fabricated PbS CQD photoconductors by a simple fabrication process based on ligand exchange and drop cast of PbS CQD on interdigited contacts on silicon. We carried out an extensive characterization in terms of responsivity and detectivity under different operating conditions and for devices of different geometrical dimensions.

The overall performance obtained at low voltage bias, combined with the simple fabrication process, make the proposed devices suitable for applications as low-cost NIR photodetectors, despite some minor drawbacks, such as the nonlinear response and the dark current fluctuations.

REFERENCES

De Iacovo, A., Venettacci, C., Colace, L., Scopa, L., Foglia, S. (2016). PbS Colloidal Quantum Dot Photodetectors operating in the near infrared. *Scientific Reports*, 6, 37913.

De Iacovo, A., Venettacci, C., Colace, L., Scopa, L., Foglia, S. (2017). High Responsivity Fire Detectors Based on PbS Colloidal Quantum Dot Photoconductors. *IEEE Photonics Technology Lett*ers, 29, 703-706.

De Iacovo, A., Venettacci, C., Colace, L., Scopa, L., Foglia, S. (2017). Noise performance of PbS colloidal quantum dot photodetectors. *Applied Physics Letters*, 111(21), 211104.

Gao, L.A, Dong, D.A, He, J.B., Qiao, K.A, Cao, F.C, Li, M.B, Liu, H.B, Cheng, Y.A, Tang, J.A., Song, H. (2014). Wearable and sensitive heart-rate detectors based on PbS quantum dot and multiwalled carbon nanotube blend film. *Applied Physics Letters*, 105(15), 153702-153705.

Gong, X.W., Yang, Z.Y., Walters, G., Comin, R., Ning, Z.J., Adinolfi, V., Voznyy, O., Sargent, E.H. (2016). Highly efficient quantum dot near-infrared light-emitting diodes. *Nature Photonics*, 10, 253-257.

Hagfeldt, A. and Grätzel, M. (1995). Light-Induced Redox Reactions in Nanocrystalline Systems. *Chemical Reviews*, 95(1), 49-68.

Kim, J.Y., Voznyy, O., Zhitomirsky, D., Sargent, E.H. (2013), 25th Aniversary Article: Colloidal Quantum Dot Materials and Devices: A quarter-century of Advances. *Advanced Materials*, 25(36), 4986-5010.

Konstantatos, G., Howard, I., Fischer, A., Hoogland, S., Clifford, J., Klem, E., Levina, L. and Sargent, E.H. (2006). Ultrasensitive solution-cast quantum dot photodetectors. *Nature*, 442, 180-183.

Konstantatos, G., Sargent, E. H. (2007). PbS colloidal quantum dot photoconductive photodetectors: transport, traps, and gain. *Applied Physics Letters*, 91(17), 173505.

Konstantatos, G., Sargent, E.H. (2009). Solution-Processed Quantum Dot Photodetectors. *Proceeding of the IEEE*, 97(10), 1666-1683.

Masini, G., Cencelli, V., Colace, L., De Notaristefani, F., Assanto. (2004). Solution-Processed Quantum Dot Photodetectors. *IEEE Journal of Selected Topics in Quantum Electronics*, 10(4), 811-815.

Moreels, I., Lambert, K., Smeets, D., De Muynck, D., Nollet, T., Martins, J.C., Vanhaecke, F., Vantomme, A., Delerue, C., Allan, G. and Hens, Z. (2009). Size Dependent Optical Properties of Colloidal PbS Quantum Dots. *ACS Nano*, 3(10), 3023-3030.

Murray, C.B., Noms, D.J. and Bawendi, M.G. (1993). Synthesis and Characterization of Nearly Monodisperse CdE(E=S, Se, Te) Semiconductor Nanocrystallites. *Journal of American Chemical Society*, 115(19), 8706-8715.

García De Arquer, F.P., Lasanta T., Bernechea, M., Konstantatos, G. (2015). Tailoring the Electronic Properties of Colloidal Quantum Dots in Metal–

Semiconductor Nanocomposites for High Performance Photodetectors. *Small*, 11, 2636-2641.

García De Arquer, F.P., Armin A., Meredith, P., Sargent, E.H.. (2017). Solution-processed semiconductors for next-generation photodetectors. *Nature Reviews Materials*, 2(3), 1-16.

Saran, R., Curry, R.J. (2016). Lead sulphide nanocrystal photodetector technologies. *Nature Photonics*, 10(2), 81-92.

Stivala, S., Pasquazi, A., Colace, L., Assanto, G., Busacca, A., Cherchi, M., Riva Sanseverino, S., Cino, A., Parisi, A (2007). Guided-wave frequency doubling in surface periodically poled lithium niobate: Competing effects. *Journal of the Optical Society of America B*, 24(7), 1564-1570.

Venettacci, C., Colace, L., Scopa, L., Foglia, S. (2017). PbS colloidal quantum dot visible-blind photodetector for early indoor fire detection. *IEEE Sensors Jornal*, 17(14), 4454-4459.

Voznyy, O., Zhitomirsky, D., Stadler, P., Ning, Z., Hoogland, S., Sargent, E.A. (2012). A charge-orbital balance picture of doping in colloidal quantum dot solids. *ACS Nano*, 6(9), 8448-8455.

Weidman, M.C., Beck, M.E., Hoffman, R.S., Prins, F., Tisdale, W.A. (2014). Monodisperse, air-stable PbS nanocrystals via precursor stoichiometry control. *ACS Nano*, 8(6), 6363-6371.